35th Annual International Conference of the IEEE EMBS
Osaka, Japan, 3 - 7 July, 2013

System Development and Performance Evaluation on Detection Schemes for UWB-IR Implant Communications

Kenta Katsu, Daisuke Anzai, *Member, IEEE* and Jianqing Wang, *Member, IEEE*

***Abstract*— Ultra wideband-impulse radio (UWB-IR) transmission is one of promising transmission technologies in implant body area networks (BANs). Although some studies have investigated the channel model and communication architecture in implant BANs, no study quantitatively shows the feasibility of UWB-IR communication in the human body with actual developed transceivers at a high data rate. In this paper, we focus on experimental evaluation of the correlation detection (coherent detection) and the energy detection (non-coherent detection) for UWB-IR transmission with multi-pulse position modulation (MPPM). For this purpose, we develop a UWB-IR communication system with MPPM scheme, and experimentally evaluate the transmission performance of the developed systems with the two different detection schemes. In addition to the experimental evaluation, we also theoretically analyze the bit error rate (BER) performance by using Gaussian approximation. From the experimental results, the developed system has achieved a BER of 10^{-2} at the propagation loss of 75 dB with a data rate of 2Mbps in the correlation detection. This result shows the feasibility of reliable UWB-IR communication in actual implant BANs.**

I. INTRODUCTION

In recent years, wireless body area networks (BANs) are becoming a reality with the development of ubiquitous society. Wireless BAN is a technology which transmits data over a short distance around the human body, and the applications of wireless BANs are expected in the field of medical and health care such as patient monitoring and medical treatment [1]. Wireless BANs are classified as wearable BANs and implant BANs due to the difference in the propagation routes and applications. Especially, implant BANs communicate between the inside and outside of the human body, and the wireless capsule endoscopy (WCE) has been one of the most important applications [2][3]. WCE is a small capsule swallowed by the patient, which consists of a color camera, radio telemetry transmitter, battery and antenna etc., and transmits the picture of the digestive system to the outside of the human body [2]. In [3], currently reported WCE techniques are summarized. All of them employ 400 MHz, 2.4 GHz or dozens of MHz band, and narrow-band modulation schemes such as FSK or BPSK. As a result, the data rate is limited mainly in the order of several hundred kbps. However, in view of the WCE application, for example, a higher data rate is required for a real-time image and video transmission.

In order to solve such a problem, we focus on the low-band ultra wideband (low-band UWB) transmission technique. As for UWB transmission schemes, UWB-impulse radio (UWB-IR), direct UWB (DS-UWB), and multiband-orthogonal frequency division multiplexing (multiband-OFDM) have been suggested [4]-[6]. For the UWB transmission schemes, we pay attention to the UWB-IR system. This is because UWB-IR can accomplish low power consumption and high data rate with an extremely short pulse.

In implant communication on UWB-IR, channel modeling and communication architecture have been reported [7]-[9]. However, no study quantitatively shows the feasibility of UWB-IR communication in the human body with actual developed transceivers at a high data rate. To show the feasibility of UWB-IR communication in the human body, it is important to optimally choose a detection scheme of UWB-IR signals. Thus, this paper experimentally evaluates the BER performances with respect to the propagation loss for the energy detection and the correlation detection in UWB-IR communication. For this purpose, we first develop a UWB-IR communication system with a multi-pulse position modulation (MPPM). Then, we theoretically analyze the BER performance of the two detection schemes by using the Gaussian approximation. In addition to the theoretical analyses, we also derive the BER performances for the two detection schemes experimentally. Finally, we compare the two results, and clarify the communication feasibility of the energy detection and correlation detection for UWB-IR transmission in the human body.

II. UWB-IR SYSTEM MODEL

A. Tranceiver

Fig.1 shows the block diagram of the transmitter system. In this paper, as a UWB-IR pulse, we use the first order Gaussian monocycle pulse, which is given by

$$\begin{aligned} p(t) &= \frac{d}{dt}\left[E_n \exp\left(-\frac{2\pi}{\tau^2}t^2\right)\right] \\ &= -E_n \frac{4\pi t}{\tau^2}\exp\left(-\frac{2\pi}{\tau^2}t^2\right) \end{aligned} \quad (1)$$

where E_n and τ are the constants determined by the overall radiated power level and the pulse width parameter which controls bandwidth B, respectively. With this pulse, the transmitter uses an MPPM scheme. This modulation scheme transmits information by the time position of several pulses. The block of the MPPM controls the time delay which can be configurable. Also, the time delay determines when the pulse generator is triggered. As explained above, in the MPPM, power amplifiers are not needed. Also, carrier is not required in the modulation. Assuming K as the total number

K. katsu, D. Anzai and J. wang are with Graduate School of Engineering, Nagoya Institute of Technology, Nagoya 466-8555, Japan. e-mail: cjk17528@stn.nitech.ac.jp, {anzai, wang}@nitech.ac.jp.

978-1-4577-0216-7/13/$26.00 ©2013 IEEE

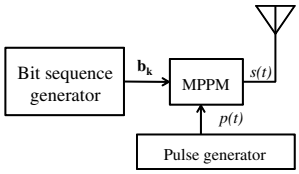

Fig. 1. Structure of transmitter

of transmitted bits, the waveforms of the MPPM signal $s(t)$ can be written as

$$s(t) = \sum_{i=1}^{K} \mathbf{b}_i^T \mathbf{p}\big(t - (i-1)T_s\big) \tag{2}$$

where $\mathbf{b}_i$ and T_s are i-th transmitted bit information vector, which denote $\mathbf{b}_i \in \{\mathbf{b}_0, \mathbf{b}_1\}$ and the symbol period, respectively, and the operator $(\cdot)^T$ expresses transpose of $(\cdot)$. Let us define L as the number of chip slots in a symbol. $\mathbf{b}_0$ and $\mathbf{b}_1$ represent a chip sequence vectors corresponding to transmitted bits of 0 and 1, respectively. These vectors are $L \times 1$ vectors.

B. Receiver

1) Energy detection: In the energy detection shown in Fig.2, since the binary MPPM chooses one from two location assignments in the k-th symbol, we calculate the energies at two locations of corresponding the k-th symbol from the received signal $r(t)$ as follows:

$$E_0^k = \sum_{l=1}^{L} b_0^l \int_{(k-1)T_s+(l-1)T_c}^{(k-1)T_s+(l-1)T_c+T_d} \big[r(t)\big]^2 dt \tag{3}$$

$$E_1^k = \sum_{l=1}^{L} b_1^l \int_{(k-1)T_s+(l-1)T_c}^{(k-1)T_s+(l-1)T_c+T_d} \big[r(t)\big]^2 dt \tag{4}$$

where T_d denotes the energy detection interval. Note that T_d is much smaller than the symbol duration T_s, and the chip slot duration T_c in UWB-IR transmission. So, T_d should be set to an appropriate time interval. By comparing E_1^k with E_0^k, we can determine the received bit information b_k as follows:

$$b_k = \begin{cases} 1 & \text{if } E_0^k > E_1^k \\ 0 & \text{otherwise.} \end{cases} \tag{5}$$

From the above equations, we emphasize that the MPPM does not require a threshold for the detection.

2) Correlation detection: In the correlation detection shown in Fig.3, we calculate the correlation between the two types of template signal for the corresponding pulse locations of the k-th symbol from the received signal $r(t)$ as follows:

$$Ec_0^k = \sum_{l=1}^{L} b_0^l \int_{(k-1)T_s+(l-1)T_c}^{(k-1)T_s+(l-1)T_c+T_d} r(t)s_0'(t)dt \tag{6}$$

$$Ec_1^k = \sum_{l=1}^{L} b_1^l \int_{(k-1)T_s+(l-1)T_c}^{(k-1)T_s+(l-1)T_c+T_d} r(t)s_1'(t)dt \tag{7}$$

where $s_0'(t)$ and $s_1'(t)$ are the template signals for each symbol, respectively. In the similar way to the energy detection, the received bit information can be determined by comparing

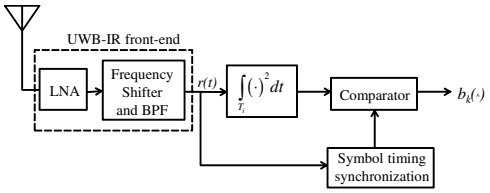

Fig. 2. Structure of receiver (energy detection)

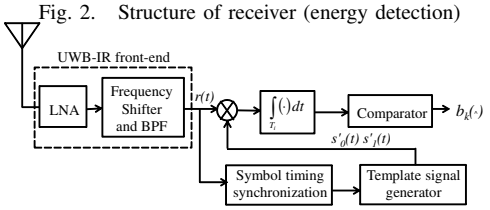

Fig. 3. Structure of receiver (correlation detection)

Ec_1^k and Ec_0^k represented as in Eq.(5). Furthermore, we assume that the symbol timing in Figs.2 and 3 is synchronized with pilot signals.

III. THEORETICAL ANALYSIS

A. Energy detection

When the transmitter sends a transmission signal $s(t)$, the received signal $r(t)$ by the receiver is expressed as

$$r(t) = s(t) + n(t) \tag{8}$$

where $n(t)$ is not a narrowband noise (in other words, it is not a Gaussian noise), because the bandpass filter (BPF) of receiver is designed for UWB-IR signals. The dimensionality of space of finite energy signals with a bandwidth B and the energy detection interval T_d can be represented about $2BT_d + 1$ [10]. Here, we approximate the $2BT_d + 1$ by an even integer $2M = 2BT_d$ for the mathematical convenience. Since the UWB-IR signals are extremely broadband, the characteristic analysis is different from narrowband signals. Therefore, as shown in Fig.4, the UWB signal characteristics is analyzed by decomposing it into M narrowband signals. We take into consideration that the number of UWB pulses in each symbol is $L/2$, and substituting Eq.(8) into Eq.(3) (k is dropped without loss of generality, so E_0^k is replaced by E_d), we obtain [11]

$$\begin{aligned} E_d &= \sum_{l=1}^{L} b_0^l \int_{(l-1)T_c}^{(l-1)T_c+T_d} \big[s(t)+n(t)\big]^2 dt \\ &= \sum_{l=1}^{L/2} \int_0^{T_d} \left[\sum_{i=1}^{2M} \big(s_i^l + n_i^l\big)\phi_i(t)\right]^2 dt \\ &= \sum_{l=1}^{L/2} \sum_{i=1}^{2M} \big(s_i^l + n_i^l\big)^2 \end{aligned} \tag{9}$$

where $\phi(t)$ is the orthogonal function over the pulse interval. n_i is zero mean independent Gaussian random variables with variance $N_0/2$ and the energy E of the transmitted pulse satisfied $E = \sum_{i=1}^{2M} \big(s_i^l\big)^2$. N_0 is the noise power density. From Eq.(9), the detected energy E_d is the sum of ML independent

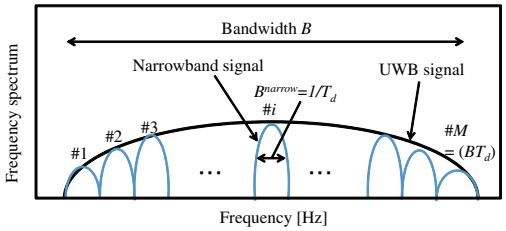

Fig. 4. Spectrum of UWB signal

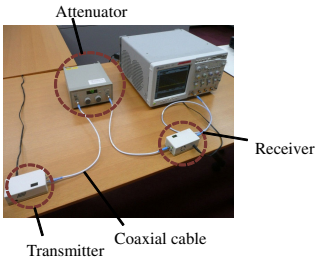

Fig. 5. View of experimental setup

variables with the chi-square distribution. According to the Central Limit Theorem, the probability density function (PDF) can be regarded as a Gaussian distribution when ML is greater. If no signal is present in the detection interval (then E=0), the mean and variance are $MLN_0/2$ and $MLN_0^2/2$. Also if the UWB signal is present, the mean and variance are $(MLN_0+LE)/2$ and $MLN_0^2/2+LEN_0$. As a result, under the Gaussian approximation, the probability of error P_e^{energy}(i.e., BER) can be written as [12]

$$P_e^{energy}\left(\frac{E_b}{N_0}\right)=Q\left(\frac{LE_b/N_0}{2\sqrt{ML+LE_b/N_0}}\right) \tag{10}$$

where E_b is the energy per bit, and $Q(x)$ is

$$Q(x)=\frac{1}{\sqrt{2\pi}}\int_x^{\infty}\exp\left(-\frac{t^2}{2}\right)dt. \tag{11}$$

B. Correlation detection

In the correlation detection, similarly to the energy detection, substituting Eq.(8) into Eq.(7), we obtain [11]

$$\begin{aligned} E_d &= \sum_{l=1}^{L} b_0^l \int_{(k-1)T_s+(l-1)T_c}^{(k-1)T_s+(l-1)T_c+T_d} r(t)s_0'(t)dt \\ &= \sum_{l=1}^{L/2}\int_0^{T_d}\left[\sum_{i=1}^{2M}\left(s_i^l+n_i^l\right)\phi_i(t)\sum_{j=1}^{2M}s_j'^l\phi_j(t)\right]dt \\ &= \sum_{l=1}^{L/2}\sum_{i=1}^{2M}\left(s_i^l+n_i^l\right)s_i'^l \end{aligned} \tag{12}$$

From Eq.(12), if no signal is present in the integration interval, the mean and variance are 0 and $LEN_0/4$. On the other hand, if the UWB signal is present, the mean and variance are $LE/2$ and $LE^2/2+LEN_0/4$. Finally, from the

TABLE I
UWB-IR TRANSMITTER PARAMETERS

Average transmit power spectrum density	-47dBm/MHz
Pulse width	100psec
Bandwith after front-end processing	120MHz
Chip time T_c	62.5nsec
Bit rate	8Mbps (L = 2) 2Mbps (L = 8)
Length of pilot signal	16 symbols
Forward error correction	None

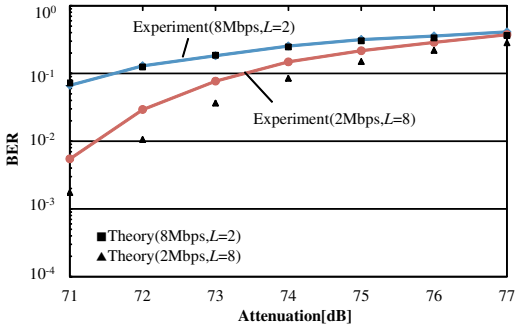

Fig. 6. BER versus attenuation performance in the energy detection

Gaussian approximation, the probability of error $P_e^{correlation}$ can be given by[12]

$$P_e^{correlation}\left(\frac{E_b}{N_0}\right)=Q\left(\sqrt{\frac{LE_b}{2N_0}}\right). \tag{13}$$

IV. TRANSEMITTION PERFORMANCE EVALUATION

A. Setup of experiment

In addition to theoretical analyses, we conducted experimental evaluation of the transmission performance for the energy and correlation detection. In this experiment, we attenuated the signal by using an attenuator to control the attenuation between the transceiver. Fig.5 shows the experimental setup. The data rate of transmitter was either 8 Mbps ($L=2$) or 2 Mbps ($L=8$). We calculated the BER from comparison between the transmitted bit sequence and the received bit sequence which was demodulated by the two detections. In order to synchronize the symbol timing at the receiver, we determined the appropriate length of the pilot signals in advance. Finally, the experimental parameters of the UWB-IR transmitter in this experiment are summarized in Table 1.

B. Results

Figs. 6 and 7 show the measured and analyzed average BER performances of the energy detection and the correlation detection as a function of the attenuation between the transmitter and receiver. From Figs.6 and 7, we emphasize that the experimental and theoretical results for the both detection methods are in good agreement due to the precise

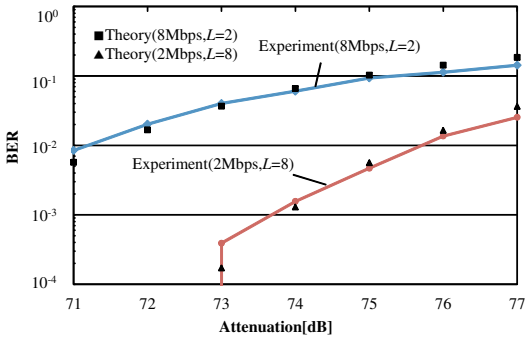

Fig. 7. BER versus attenuation performance in the correlation detection

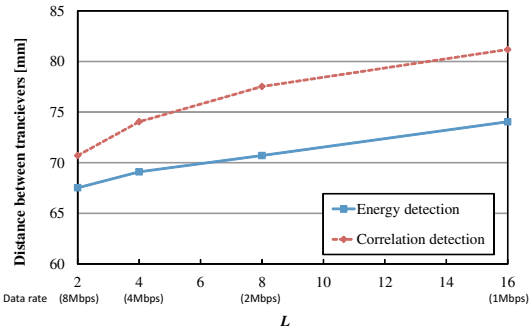

Fig. 8. Communication distance versus slot number L or data rate

symbol timing synchronization of the developed UWB-IR communication system.

Comparing the results of the energy detection and correlation detection at the BER performance of around 10^{-2} in Figs.6 and 7, the BER performance of the correlation detection is found to be about 3 dB better than that of the energy detection at the data rate of 8 Mbps. Furthermore, the developed UWB-IR communication system in the correlation detection can achieve the BER performance of less than 10^{-2} until the attenuation of 75 dB at the data rate of 2 Mbps. According to [9], the path loss model in a capsule endoscope situation can be expressed by the following equation:

$$PL_{dB} = PL_{0,dB} + 10n\log_{10}\left(\frac{d}{d_0}\right) + S_{dB} \qquad (14)$$

where $PL_{0,dB}$ is the path loss at the reference distance d_0, d is the distance between the inside capsule and the outside receive antenna, n is the pass loss exponent, and S_{dB} is the shadow fading. In [9], the parameters in Eq.(14) is obtained as $PL_{dB,0} = 48.1$ dB at $d_0 = 5$ cm, $n = 10$ and $S_{dB} = 7.85$ dB, at a typical receiver position. Using Eq.(14), we calculated the distance between the transceiver at the BER of 10^{-2}. The results are shown in Fig.8. We can see from this figure that the energy detection and the correlation detection can establish a reliable communication at the distance of nearly 7 cm and 8 cm, respectively, at most, with the data rate of 2 Mbps. This result indicates the feasibility of UWB-IR communication in real implant BANs, because this communication distance almost covers the deepest place of the human body.

V. CONCLUSIONS

For realizing a high-speed and reliable UWB-IR communication in implant BANs, we have developed a UWB-IR communication system with an MPPM scheme, and the energy detection and correlation detection. Then, we have evaluated the BER performance of the developed UWB-IR system for the two detection methods, both analytically and experimentally. From the experimental and analytical results, the developed system can achieve a BER of 10^{-2} at the attenuation of 72 dB for energy detection and 75 dB for correlation detection with a data rate of 2 Mbps. Through linking the attenuations to our previously derived path loss, we have shown that the UWB-IR with energy detection and correlation detection can establish a communication distance up to nearly 7 cm and 8 cm in a WCE channel, respectively, at the data rate of 2 Mbps. This result has indicated the feasibility of reliable implant BAN communication in a reality.

Our future subjects are to further improve the performance of the developed UWB-IR system and to evaluate it via a living body experiment.

REFERENCES

[1] E. Monton, J.F. Hernandez, T. Herve, J. Micallef, I. Grech, A. Brincat and V. Traver "Body area network for wireless patient monitoring," *IET Communications*, vol. 2, no. 2, pp. 215-222, Feb. 2008

[2] G. Iddan, G. Meron, A. Glukhovsky and P. Swain, "Wireless capsule endoscopy," *Nature*, vol. 405, pp. 417, May. 2000

[3] M. R. Yuce, T. Dissanayake, and H. C. Keong, "Wireless telemetry for Electronic Pill Technology" *IEEE Sensors*, pp. 1433-1438, Oct. 2009

[4] M. Z., Win and R. A. Scholtz, "Ultra-wide band time-hopping spread spectrum impulse radio for wireless multiple-access communications," *IEEE Trans. commun.*, vol. 48, pp. 679-691, Apr. 2000

[5] P. Runkle, J. McCorkle, T. Miller, and M. Welborn, "DS-CDMA: The modulation technology of choice for UWB communications," in *Proc. IEEE Conf. Ultra Wideband Systems and Technologies (UWBST'03)*, Reston, VA, Nov. 2003 pp. 364-368

[6] J. Balakrishnan, A. Batra, and A. Dabak, "A multi-band OFDM system for UWB communication," in *Proc. IEEE Conf. Ultra Wideband Systems and Technologies (UWBST'03)*, Reston, VA, Nov. 2003, pp. 354-358

[7] R. Chavez-Santiago, A. Khaleghi, I. Balasingham and T. A. Ramstad, "Architecture of an ultra wideband wireless body area network for medical applications," *Presented at 2nd Int. Symp. on Applied Sciences in Biomedical and communication Tech.*, Nov. 24-27, 2009, Bratislava, Slovak.

[8] J. Wang and Q. Wang, "Channel Modeling and BER Performance of an implant UWB Body Area Link," *Presented at 2nd Int. Symp. on Applied Sciences in Biomedical and Communication Tech.*, Nov. 24-27, 2009, Bratislava, Slovak.

[9] J. Shi, D. Anzai and J. Wang, "Channel modeling and performance analysis of diversity reception for implant UWB wireless link," *IEICE Trans. Commun.*, vol. E95-B, no. 10, pp. 3197-3205, Oct. 2012

[10] P.A. Humblet, and M. Azizoglu, "On the Bit Error Rate of Lightwave Systems with Optical Amplifiers," *Journal of Lightwave technology*, vol. 9, no. 11, Nov. 1991

[11] S. Dubouloz, B. Denis, S. de Rivaz and L. Ouvry, "Performance Analysis of LDR UWB Non-Coherent Receivers in Multipath Environments," in *Proc. IEEE International Conference on Ultra-Wideband*, pp. 491-496, Sep. 2005

[12] J. G. Proakis and M. Salehi, *Digital Communications.* McGraw-Hill, 2008